

SPATIAL AND TEMPORAL DISTRIBUTION OF IONOSPHERIC CURRENTS - 4: ALTITUDE-LOCAL TIME AND ALTITUDE-LONGITUDE CROSS SECTIONS OF EQUATORIAL ELECTROJET CURRENT DENSITY.

C. AGODI ONWUMECHILI, S. O. OKO and P. O. EZEMA

(Received 12 January 2001; Revision accepted 25 October 2001)

ABSTRACT

The rare opportunity given by the unprecedented spatial and temporal coverage of POGO satellites data is exploited to present all possible cross sections of equatorial electrojet (EEJ) current in the group of papers. Here the all-longitude means at 7 hours centred on local noon and the daytime means at 36 longitudes, of the vertical distribution parameters of EEJ current density are provided. The altitude-local time cross section of EEJ current density has one contour cell peaking at (12 h, 106 km) while the altitude-longitude cross section of EEJ current density has three contour cells peaking at (100°E, 106 km), (190°E, 106 km) and (290°E, 106 km). In both cross sections the contour of a given current density extends farther from the altitude of peak current density when the peak current density at the centre of EEJ is larger. This accounts for the wavy nature of the altitude-longitude cross section. Attention is drawn to two rocket measurements that support this phenomenon. The following conclusions are also reached. (a) The continuous distribution of current density model reproduces the altitude distribution parameters of EEJ current density very well, (b) the altitude distribution parameters of EEJ current density in India and Peru are not significantly different and (c) The altitude distribution parameters of EEJ current density from rockets data and from POGO Satellites data are not significantly different and that (d) It is essential to take into account the lack of symmetry between the vertical distributions of EEJ current density below and above the altitude of EEJ peak current density.

Key words: altitude – local time cross sections, latitude-longitude cross sections, contour cells, ionospheric currents.

INTRODUCTION

Rockets have measured many altitude profiles of equatorial electrojet (EEJ) current density Onwumechili (1992 a, b, c, d and e) made a comprehensive study of them. Unfortunately, a rocket measures the profile at only one location in a brief period and the experiment is somewhat expensive. Consequently only very few locations have been covered by all the experiments and it is unusual to launch more than one or two successful rockets in a day. Therefore, rocket measurements at affordable costs are not suitable for the construction of spatial and temporal distribution of ionospheric currents. Indeed, we are not aware of any publication of altitude-local time and altitude-longitude cross sections of EEJ current density.

Fortunately, the POGO satellites measured the magnetic fields of the EEJ from 1967 to 1969. They covered all latitudes and longitudes within the EEJ zone at varying altitudes and from about 09 hr to 15 hr local time. It follows that if EEJ current density is derived from the POGO data with a thick current shell model, it becomes possible to produce all the cross sections of EEJ current density. It is this rare opportunity that is being exploited by this group of papers. The thick current shell model employed is briefly introduced below.

In the continuous distribution of current density model (Onwumechili 1965) the eastward current density j at the point (x, z) is given by

$$j = j_0 \frac{a^2(a^2 + \alpha x^2)b^2(b^2 + \beta z^2)}{(a^2 + x^2)^2(b^2 + z^2)^2} \dots\dots\dots 1$$

where x is northward latitude, z is downward vertical distance, j_0 is the peak current density at the current centre $x = 0 = z$, a is scale latitude, b is vertical scale length, and α and β are dimensionless parameters controlling current distribution latitudinally and vertically respectively.

The Eq. (1) may be re-written as

$$j = C_0 \frac{b^2(b^2 + \beta z^2)}{(b^2 + z^2)^2} \quad \dots\dots\dots 2$$

where

$$C_0 = j_0 \frac{a^2(a^2 + \beta x^2)}{(a^2 + x^2)^2} \quad \dots\dots\dots 3$$

Thus c_0 is the peak current density at x^0 dip latitude such as the location of a rocket launching. It occurs at the point. $(x, 0)$. If $z = p$ at the altitude where $j = \frac{1}{2}c_0$, Eq. (2) gives

$$p^2 = b^2 [(\beta - 1) + \sqrt{1 + (\beta - 1)}] \quad \dots\dots\dots 4$$

Thus the parameter p measures half of the vertical thickness of the EEJ between the altitudes where its density j is half of its peak current density C_0 . This is easily measurable from altitude profiles of j measured by rockets.

This model fits extremely well the altitude profiles of ionospheric currents measured by rockets. The excellent fitting is demonstrated by Fig. 1 from Onwumechili (1992e). The deviations of the calculated from the observed points in Fig. 1 (a) have a mean of -0.010 Error! Not a valid link. 0.353, a median of -0.006 , a mean magnitude of 0.269 ± 0.223 and root-mean-square (rms) of 0.347 Akm^{-2} .

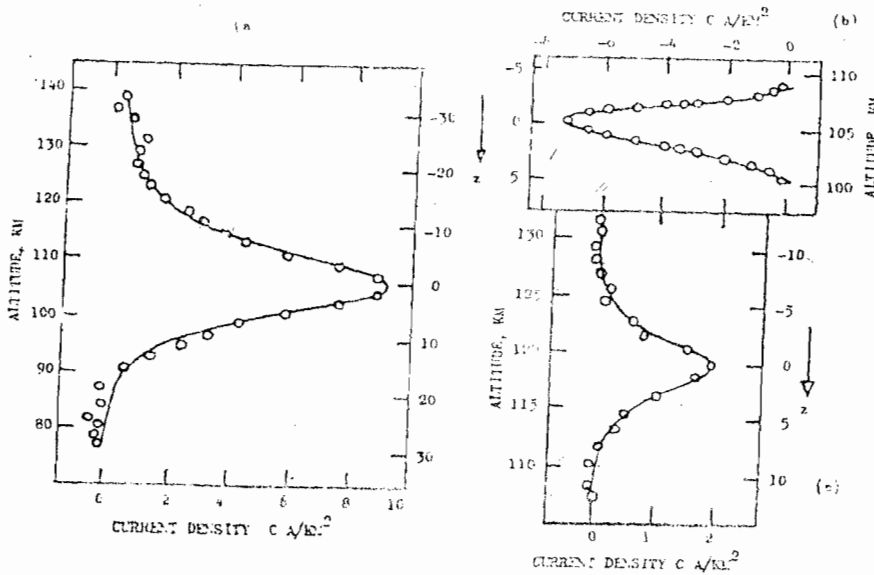


Fig. 1 The continuous distribution of current density model fittings of the altitude profiles of current density $C \text{ Akm}^{-2}$ observed during rocket flights: (a) the equatorial electrojet of Sastry's (1970) flight 20.06 from -0.47° dip latitude at 1045 hr L.T., (b) the reverse westward current of Cahill's (1959) flight SUI 83 from 537 km dip distance at 1424 hr L.T., and (c) the upper current layer on the descent of Maynard's (1967) flight UNH 65-2 from 8° dip latitude at 1214 hr. L.T. The points are observed by rockets and the smooth curves are calculated from the model. After Onwumechili (1992e).

Some 25 vertical profiles of EEJ in all were fitted. The differences of their calculated peak current densities C_0^c from their observed C_0^o have a mean of 0.009 ± 0.223 , a median of -0.013 , a mean magnitude of 0.173 Error! Not a valid link. 0.142 and a rms of 0.222 Akm^{-2} . The differences of their calculated half thickness p^c from their observed half thickness p^o have a mean of -0.022 Error! Not a valid link. 0.233, a median of 0.019 , a mean magnitude of 0.173 Error! Not a valid link. 0.156, and a rms of 0.231 km .

To achieve the above, Onwumechili (1992e) fitted separately, the lower part of the profile below the altitude of the peak and the upper part of the profile above the altitude of the peak current density because

the profiles are not symmetrical about the altitude of the peak current density. There is no doubt that the model is appropriate for the study of vertical distribution of ionospheric currents.

CALCULATION OF THE CROSS SECTIONS

The altitude-local time and altitude-longitude cross sections of EEJ current density j - Akm^{-2} involve the calculation of altitudes

$$h = h_e - z \quad \dots\dots\dots 5$$

where a selected current density occurs. Here h_e is the altitude of the current centre where $z=0$. For this purpose Eq. (2) may be written as

$$p = \frac{1 + \beta s^2}{(1 + s^2)^2} \quad \dots\dots\dots 6$$

where the ration $\rho = j/C_0$ and the reduced distance $s = z/b$. The solution of Eq. (6) for s or z is

$$z^2 = b^2[(\beta - 2\rho) \pm \sqrt{(\beta - 2\rho)^2 - 4\rho(\rho - 1)}] / 2\rho \quad \dots\dots\dots 7$$

It emerges that for the altitude-local time and altitude-longitude cross sections, the following parameters are needed: b , β , j_0 , half thickness p , h_e and L_2 .

The altitude of the EEJ current centre h_e km cannot be derived from the magnetic field of the current. It is measured by rockets which penetrate through the current centre to higher altitudes. The mean from 23 rocket altitude profiles of j studied by Onwumechili (1992cd) is $h_e = 106 \pm 1$ km. The 23 profiles include 14 within 0° to 2° , 6 within the transition zone of 2° to 4° , and 3 in the return current zone of within 4° to 7° dip latitude. Thus the altitude $h = 106-z$ km.

The altitude extent of the current from $-L_2$ to L_2 km is difficult to determine exactly. The extent L_2 can be measured from the altitudes where the rocket begins to and ceases to find current. However, this depends on the sensitivity of the sensors on board the rocket. The more sensitive the sensors the larger the L_2 . It can also be decided *a priori* that the altitude extent of a certain current density contour be regarded as the altitude extent of the current. This would be arbitrary. However, a reasonable estimate of L_2 can be made in a given circumstance.

The other parameters of the model are derived from fitting the magnetic fields of the current. The current density j of Eq. (1) is put into Biot-Savart law. On integrating latitudinally through the extent from $-L_1$ to L_1 and vertically from $-L_2$ to L_2 , expressions are obtained for the northward X and vertical Z components of the magnetic field of the current (Onwumechili 1966). These expressions for X and Z contain the model parameters j_0 , a , α , b , and β which may therefore be obtained by fitting the magnetic fields.

The POGO satellites data of 1967 - 1969 are fitted with the magnetic field expressions to obtain these parameters of the model (Onwumechili *et al.* 1992). With these parameters of the model, nearly all the physical parameters concerning the spatial distribution of EEJ current can be calculated. A comprehensive analysis of the POGO data yielded 894 values of each parameter. For each parameter, these values are organized into a table of 36 longitude rows for 0° , 10° , 20° ... $350^\circ E$ and 7 local time hour columns for 09, 10, 11... 15 hour. This applies also to the desired parameters b , β , j_0 and half thickness p .

ALTITUDE-LOCAL TIME CROSS SECTION OF EQUATORIAL ELECTROJET CURRENT DENSITY

The columns of the longitude-local time tables of b , β , j_0 and p are averaged to get their all-longitude means for each local time hour as given in Table 1. The altitude-local time cross section is set on the vertical plane $x = \text{constant}$. The altitude is measured vertically and local time is measured eastwards. It is convenient to start with the case of the plane $x = 0$. This is the dip equatorial plane through the axis of EEJ. In this case the C_0 of Eq. (3) is j_0 , the peak current centre. But this peak current density j_0 at a given time depends on longitude. For convenience we start with the all-longitude mean of j_0 . Accordingly, the corresponding parameters must all be the all-longitude means. These are given in Table 1.

Suppose it is decided to construct the contour of the current density $j = 4 \text{ Akm}^{-2}$. For a selected local time hour t , the values of $p = 4/j_0$, b and β from Table 1 are substituted in Eq. (7). Two equal and opposite values of z are obtained, one below and one above the altitude of the peak current density. This is repeated for other local time hours with $p = 4/j_0$ but j_0 takes its appropriate value for each local time. All the solutions for z using $p = 4/j_0$ for all the local time hours are then joined with a smooth curve to get the contour of $j = 4 \text{ Akm}^{-2}$. In the same way other desired contours are constructed.

Table 1 Average values, from all longitudes, of certain parameters of equatorial electrojet current, derived from POGO satellites data of 1967 – 1969, necessary for altitude-local time cross section.

| Local Time Hour. | Scale Length b km | Distribution Parameter β | Current Density $j_0 \text{ A/km}^2$ | Vertical Thickness p km |
|------------------|---------------------|--------------------------------|--------------------------------------|---------------------------|
| 09 | 8.8722 | 0.5341 | 5.930 | 7.17 |
| 10 | 9.0968 | 0.5496 | 8.412 | 7.32 |
| 11 | 8.9214 | 0.5000 | 9.329 | 7.05 |
| 12 | 8.8451 | 0.5253 | 10.439 | 7.05 |
| 13 | 9.0760 | 0.5350 | 8.005 | 7.26 |
| 14 | 9.1516 | 0.5274 | 6.689 | 7.30 |
| 15 | 8.7892 | 0.5188 | 4.480 | 7.00 |
| Mean | 8.9641 | 0.5270 | 7.612 | 7.16 |
| S.D. | 0.1416 | 0.0153 | 2.050 | 0.13 |

The resulting altitude-local time cross section is given in Fig. 2. It shows contours of 10, 8, 6, 4, 3, 2, 1, 0.5 and 0.1 Akm^{-2} . It assumes that the contours are symmetrical about the altitude of the peak current density. We know that this is not correct but the POGO data affords no opportunity for fitting the upper and lower parts separately as Onwumechili (1992e) did for rocket profiles. Contours outside 09 hr to 15 hr are extrapolations.

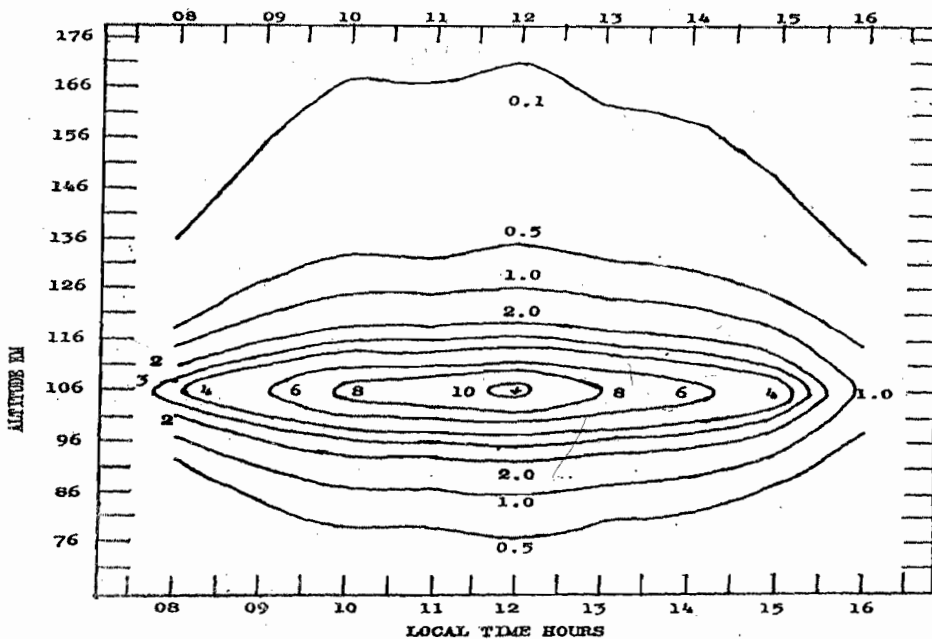


Fig. 2 Altitude-local time cross section of equatorial electrojet current density $j \text{ Akm}^{-2}$ showing contours of 10, 8, 6, 4, 3, 2, 1, 0.5 and 0.1 Akm^{-2} . Symmetry about the altitude of peak current density is assumed. Contours outside 09 to 15 hr local time are extrapolations.

Fig. 2 shows that along a given altitude the current density increases from morning to a maximum around local noon and then decreases towards evening.

When the cross section is set on the vertical plane $x = a$ constant $\neq 0$, the value of $C_0 < j_0$ is found from Eq. (3) using the appropriate values of a and α . Then the ratio $p = j/C_0$. The resulting cross section has the

same pattern as Fig. 2 but the current density is reduced everywhere on the cross section relative to the density on Fig. 2. When the parameters for a selected longitude are used for constructing the cross section, the pattern is the same as in Fig. 2. However, the current density on the cross section is higher or lower than that at the corresponding point on Fig. 2 according as the peak current density for the selected longitude is higher or lower than the all longitude mean j_0 used for Fig. 2.

The major general feature of the cross section is that the contour of a given current density extends to a greater altitude at a time when the current is more intense at its centre. This feature may be explained as follows. At a given location and given time, the EEJ current density decreases with altitude away from its peak current density at the current centre. As the EEJ intensifies from morning towards local noon, its current density increases at all altitudes. Arising from this a given current density occurs at a higher altitude when the peak current density at the current centre is greater.

This may be illustrated as follows. At 0900 local time the peak current density at the current centre is 5.9 Akm^{-2} and the density of 2 Akm^{-2} occurs at a height of 9.7 km. above the altitude of the centre. By 1000 L.T. the peak current density at the current centre increases by a factor of 1.424 to 8.4 Akm^{-2} . If the current density at all altitudes were to increase by the same factor, at 1000 L.T. the current density at 9.7 km above the current central axis would be 2.85 Akm^{-2} , which is close to the actual value of 3 Akm^{-2} . Thus this main feature of Fig. 2 is the natural consequence of the decreasing current density of the EEJ with distance away from its centre coupled with the growth of the current density everywhere from morning towards local noon. At a given local time, the current increases, from its lower edge, with increasing altitude to a maximum at the altitude $h_e = 106 \text{ km}$, and thereafter it decreases with altitude monotonically. Arising from these variations with altitude and local time, a big contour cell peaks at (12 h, 106 km).

ALTITUDE-LONGITUDE CROSS SECTION OF EQUATORIAL ELECTROJET CURRENT DENSITY

The altitude-longitude cross section of EEJ current density is set on the vertical plane $x = \text{constant}$ with altitude on the vertical axis and longitude on eastward axis. We first consider the case of the dip equatorial plane $x = 0$, through the centre of EEJ. It is clear from Eq. (3) that in this case $C_0 = j_0$, the peak current density at the current centre. But this peak j_0 also depends on local time. We choose to start with the daytime mean j_0 based on the average from 09 hr to 15 hr local time. This is obtained by averaging the rows of the longitude-local time matrix table of j_0 . The daytime means of the other necessary parameters are similarly obtained. These are given in Table 2.

To construct the contour of current density $C = 2 \text{ Akm}^{-2}$ for example, the values of $p = 2/j_0$, b and β appropriate for a selected longitude in Table 2 are inserted in Eq. (7). The two solutions for z are noted. Solutions for z are similarly obtained for all the 36 longitudes in Table 2. These values for z are plotted, and the smooth curve through them is the contour of $C = 2 \text{ Akm}^{-2}$. In the same way all the desired contours are constructed.

The resulting altitude-longitude cross section of EEJ current with contours of 10, 8, 6, 4, 3, 2, 1, 0.5 and 0.1 Akm^{-2} is given in Fig. 3. It has already been mentioned that the assumption of symmetry about the altitude of the peak current density is not wholly justified by observations. The EEJ current is observed to extend more above the altitude of the peak current density than below it. However, the POGO data is not appropriate for taking the asymmetry into account.

Fig. 3 shows that along a given meridian of longitude, the EEJ current density increases with altitude to a maximum at the altitude of the centre of EEJ at about 106 km altitude. Thereafter, the current density decreases with altitude. At a fixed altitude the EEJ current density has maxima at about 100°E , 190°E and 290°E , and minima at about 145°E and 230°E . Arising from these variations of current density, the cross section displays three contour cells with peaks at (100°E , 106km), (190°E , 106 km) and (290°E , 106 km).

When the contour is set on the vertical plane $x = \text{constant} \neq 0$, we see from Eq. (3) that the peak current density $C_0 < j_0$. Consequently, the pattern of the resulting cross section remains the same as in Fig. 3. but the current density is reduced everywhere relative to Fig. 3. In place of the day time means of the parameters j_0 , b and β , their values at a selected local time may be used to construct the altitude-longitude cross section of EEJ current density. In that case the pattern of the cross section will be the same as in Fig.

Table 2 Daytime average values, from 09 hr to 15 hr, of certain parameters of equatorial electrojet current, derived from POGO satellites data of 1967 - 1969, necessary for altitude-longitude cross section.

| Longitude Degree East | Scale Length b km | Distribution Parameter β | Current Density j_0 A/km ² | Vertical Thickness km p |
|-----------------------|-------------------|--------------------------------|-----------------------------------------|---------------------------|
| 0 | 8.9583 | 0.5212 | 5.996 | 7.14 |
| 10 | 9.0082 | 0.5233 | 4.895 | 7.17 |
| 20 | 9.0701 | 0.5361 | 4.576 | 7.23 |
| 30 | 9.1005 | 0.5324 | 4.946 | 7.28 |
| 40 | 9.1194 | 0.5234 | 5.134 | 7.27 |
| 50 | 9.2083 | 0.5195 | 4.857 | 7.34 |
| 60 | 8.8816 | 0.5192 | 5.054 | 7.07 |
| 70 | 8.6599 | 0.5141 | 6.918 | 6.99 |
| 80 | 8.3766 | 0.5139 | 9.531 | 6.65 |
| 90 | 8.8660 | 0.5310 | 10.964 | 6.95 |
| 100 | 9.0927 | 0.5438 | 11.439 | 7.30 |
| 110 | 9.0290 | 0.5484 | 9.752 | 7.26 |
| 120 | 8.9636 | 0.5525 | 7.877 | 7.22 |
| 130 | 8.9594 | 0.5486 | 5.127 | 7.21 |
| 140 | 9.0361 | 0.5437 | 4.795 | 7.26 |
| 150 | 9.0001 | 0.5283 | 4.892 | 7.20 |
| 160 | 8.8761 | 0.5197 | 6.432 | 7.07 |
| 170 | 8.7664 | 0.5164 | 8.178 | 6.98 |
| 180 | 8.7369 | 0.5210 | 10.041 | 6.96 |
| 190 | 8.7638 | 0.5202 | 10.583 | 6.97 |
| 200 | 8.8767 | 0.5231 | 9.020 | 7.07 |
| 210 | 8.9482 | 0.5251 | 7.213 | 7.13 |
| 220 | 8.9522 | 0.5302 | 5.938 | 7.15 |
| 230 | 8.8096 | 0.5231 | 5.951 | 7.05 |
| 240 | 8.8881 | 0.5252 | 6.390 | 7.09 |
| 250 | 9.0430 | 0.5229 | 7.470 | 7.21 |
| 260 | 9.0381 | 0.5260 | 8.480 | 7.21 |
| 270 | 9.1241 | 0.5350 | 10.114 | 7.30 |
| 280 | 9.0145 | 0.5423 | 11.199 | 7.25 |
| 290 | 9.0435 | 0.5413 | 12.415 | 7.34 |
| 300 | 9.1473 | 0.5336 | 11.712 | 7.34 |
| 310 | 9.0614 | 0.5177 | 10.102 | 7.21 |
| 320 | 9.0906 | 0.5047 | 7.801 | 7.20 |
| 330 | 9.0708 | 0.5077 | 6.212 | 7.19 |
| 340 | 9.1496 | 0.5218 | 5.981 | 7.28 |
| 350 | 8.9547 | 0.5203 | 6.044 | 7.12 |
| Mean | 8.9635 | 0.5270 | 7.627 | 7.15 |
| S.D. | 0.1625 | 0.0119 | 2.423 | 0.15 |

3 but the current density everywhere on it will be higher or lower relative to Fig. 3 according as the peak current density at the selected local time is higher or lower than the daytime mean j_0 used in constructing Fig. 3.

A striking feature of the altitude-longitude cross section of EEJ current density is the wavy nature of the contours. This is basically the same phenomenon of a given contour extending farther in altitude when the peak current density at the current centre is larger. Thus a given contour rises in altitude as the longitude of current maximum is approached. It falls in altitude as the longitude of current minimum is approached. After the longitude of the minimum it again rises in altitude towards the longitude of the next maximum current. This explains the waviness of the contours with peak altitudes at the longitudes of maximum current density at 100°E, 190°E and 290°E, and trough altitudes at the longitudes of current density minimum at 145°E and 230°E.

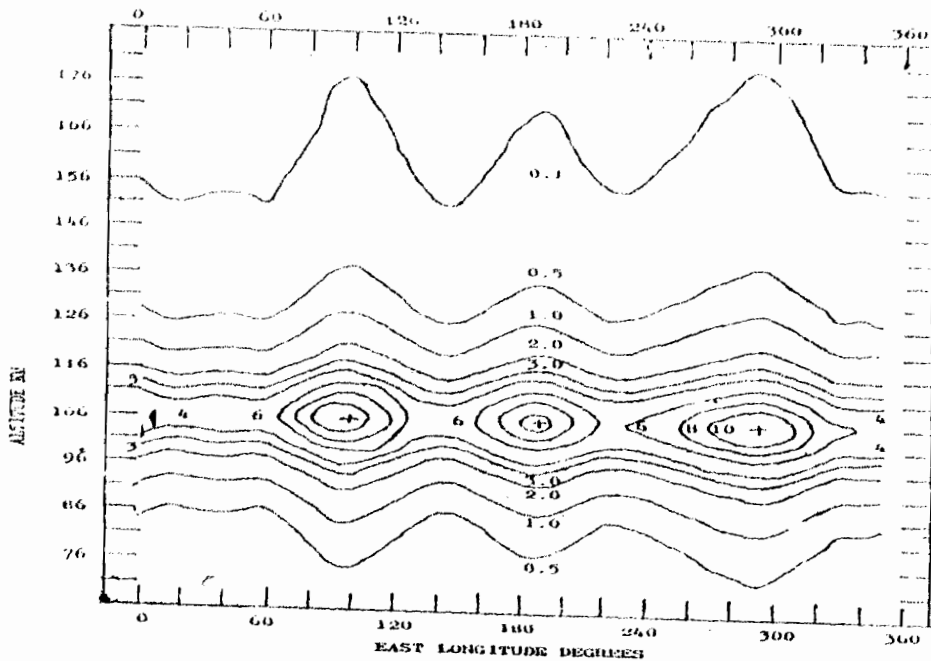


Fig. 3 Altitude-longitude cross section of equatorial electrojet current density j Akm^{-2} showing contours of 10, 8, 6, 4, 3, 2, 1, 0.5 and 0.1 Akm^{-2} . Symmetry about the altitude of peak current density is assumed.

DISCUSSIONS OF ALTITUDE DISTRIBUTION OF EQUATORIAL ELECTROJET CURRENT DENSITY

We are not aware of any journal publications of altitude-local time and altitude-longitude cross section of EEJ current density. There are however some publications of some altitude distribution parameters of EEJ current density related to our cross sections. Table 3 gives these parameters for India and Peru from rocket measurement. They are based on rocket measurement made within $1130 \text{ hr} \pm 2 \text{ hrs}$. The parameters in Table 3 from POGO satellites data are based on the average of 11 hr and 12 hr local time. We proceed to discuss them: firstly by comparing observed and model parameters, secondly by comparing India and Peru, and thirdly by comparing rocket and POGO satellite model parameters.

Table 3 Comparison of certain observed and model parameters of altitude distribution of equatorial electrojet current from rockets and satellites. The z_1 and z_2 are the lower and upper extents of the contour of 1 Akm^{-2} from the current centre

| Altitude Parameter | INDIA | | PERU | POGO Model | |
|----------------------------|----------|------------------|------------------|------------------|------------------|
| | Observed | Model | Observed | Model | |
| Vertical Scale Length * km | | 7.21 ± 1.61 | 8.16 ± 1.88 | | |
| Vertical Scale Length * KM | | 8.30 ± 2.05 | 7.58 ± 1.95 | | |
| Mean * KM | | 7.76 ± 1.84 | 7.87 ± 1.92 | 8.88 ± 0.26 | |
| Distribution Parameter | | 0.369 ± 0.34 | 0.024 ± 0.33 | | |
| Distribution Parameter | | 0.431 ± 0.37 | 0.391 ± 0.39 | | |
| Mean | | 0.400 ± 0.36 | 0.208 ± 0.36 | 0.513 ± 0.02 | |
| Density at Station C A/KM | 8.8 3.4 | 8.73 ± 3.6 | 9.7 ± 2.6 | 9.71 ± 2.7 | |
| Density at Equator j A/KM | | 9.42 ± 3.6 | 10.47 ± 2.3 | 9.88 ± 4.15 | |
| Lower Half Thickness p KM | 5.4 0.8 | 5.34 ± 0.78 | 5.3 ± 0.8 | 5.26 ± 0.69 | |
| Upper Half Thickness p km | 6.3 1.3 | 6.34 ± 1.30 | 5.6 ± 1.0 | 5.65 ± 0.82 | 7.05 ± 0.23 |
| Thickness | 11.7 2.1 | 11.68 ± 2.08 | 10.9 ± 1.8 | 10.91 ± 1.51 | 14.10 ± 0.46 |
| Lower Half Extent z km | | 13.93 | | 12.44 | |
| Upper Half Extent | | 16.82 | | 15.71 | 19.63 |
| Total Extent | | 30.75 | | 28.15 | 39.26 |

In his comprehensive study of rocket measurements of ionospheric currents, Onwumechili presented the observed parameters (Onwumechili, 1992c) and the model parameters (Onwumechili, 1992e) based on the continuous distribution of current density model. Both sets of parameters are available in Table 3 for the peak current density C_0 at the launching station and the half-vertical thickness p at half of the peak current density. It is seen in Table 3 that the model reproduces the observed C_0 Akm^{-2} exactly for both India and Peru.

Onwumechili (1992c) measured the half thickness at half of the peak current density separately for the lower part p_1 below the altitude of peak current density, and for the upper part p_2 above the altitude of the peak current density, because the vertical profile of EEJ current density is not symmetrical about the altitude of peak current density. For all parameters in Table 3 and for this paper, the subscript 1 refers to the lower and the subscript 2 refers to the upper part of the altitude of profile of EEJ current density.

Onwumechili (1992e) also modelled separately the lower and the upper parts of the vertical profiles of EEJ current density measured by rockets. Table 3 compares the observed and model values of p_1 , p_2 and $(p_1 + p_2)$ from rocket data of India and Peru. It is seen that the model reproduces the observed values accurately both at India and Peru. We conclude that the continuous distribution of current density model is an excellent model for the reproduction of altitude parameters of EEJ current density.

We now turn to the comparison of the altitude distribution parameters of EEJ in India and Peru. There is no significant difference between the peak current density, C_0 and j_0 , at India and Peru, but it is marginally greater in Peru than in India. The values of b_1 , b_2 and their mean b are virtually the same in India and Peru. The standard deviations of β_1 , β_2 and their mean β are very high in both India and Peru. On account of this, there is no significant difference between the values of β_1 , β_2 and β in India and Peru. However, their means are insignificantly smaller in Peru than in India.

The values of p_1 , p_2 and their sum $(p_1 + p_2)$ are virtually the same in India and Peru. The altitude extents z_1 and z_2 of the contour of $1 Akm^{-2}$ in India and Peru have been calculated with the mean values of b_1 , β_1 and b_2 , β_2 respectively. The values of z_1 , z_2 and $(z_1 + z_2)$ are correspondingly, nearly the same in India and Peru. The trend for the values at Peru to be slightly smaller than those at India is noted. However, these values are sensitively dependent on the value of β . Since the standard deviations of β_1 and β_2 are nearly equal to their means and in one case is more than 10 times the mean, the trend between India and Peru can easily be reversed. In the circumstance no reliable inference can be drawn from the trend.

We conclude that the altitude distribution parameters of EEJ current density in Table 3 are not significantly different in India and Peru. Onwumechili (1992c) suggested that the larger horizontal magnetic variation ΔH at Peru than at India often reported arises from the contribution of the upper current layer (the worldwide part of Sq) which is 2.4 times more intense at Peru than at India.

We now turn to the comparison of the altitude distribution parameters of the EEJ current density from rocket and POGO satellites observational data. There is very good agreement between the values of the EEJ peak current density j_0 from rockets and POGO satellites data. There is also good agreement between the values of the vertical scale length b from rockets and POGO satellites. Because of the large standard deviations of β_1 , β_2 and β from rockets data, the β from POGO satellites data is within the variance limits of those from rockets data but it is clearly larger than their means. It is also noted that the dispersion of the satellites β is relatively very small.

The value of the half thickness p from POGO satellites data is in good agreement with the upper half thickness p_2 from rockets data but is significantly larger than the lower half thickness p_1 . Consequently, the full vertical thickness of EEJ at half of its peak current density from POGO satellites data is close to that from rockets data in India but is significantly larger than that from rockets data in Peru.

Similarly, the upper altitude extent of the contour of $1 Akm^{-2}$ from POGO satellites data is consistent with its upper altitude extent z_2 from rockets data. Consequently, the total altitude extent $(z_1 + z_2)$ from POGO satellites data is substantially larger than that from rockets data. The substantial differences between the total thickness and the total altitude extent from POGO satellites data and rockets data are caused by the asymmetry of the vertical profiles about the altitude of the peak current density. We conclude that the vertical distribution parameters of the EEJ current density from rockets data and POGO satellites

data are not significantly different. The two cases in which there are substantial differences are caused by the asymmetry of the lower and upper distributions of EEJ current density about the altitude of its peak current density. While the asymmetry has been taken into account in the modelling of rockets data, it has not been possible to take it into account in the modeling of POGO satellites data.

We now present observational evidence in support of the phenomenon that the contour of a given current density extends higher in altitude when the peak current density at the centre of the EEJ is greater. Under quiet conditions, Maynard (1967) measured the EEJ twice from the same location above the Pacific Ocean off Peru on 12 March 1965, and Sastry (1970) observed the EEJ twice from the same location above Thumba, India, on 29 August 1968. The intense EEJ of Maynard (1967) at 1126 hr local time with peak density of 8.2 Akm^{-2} extended 13 km more than his weak EEJ at 0856 hr local time with peak density of 1.44 Akm^{-2} . Similarly, the intense EEJ of Sastry (1970) at 1045 hr local time with a peak current density of 9.4 Akm^{-2} extended 7 km more than his weak EEJ at 1352 hr local time with density 4.6 Akm^{-2} .

The lower and upper edges of a current layer detected by a rocket are likened to the contour of a certain current density because they represent the location of a certain current density which is barely detected by the sensors on board the rocket. In Paper 3 of this group, by the same phenomenon, the contours extend farther in latitude when the peak current density at the centre of the EEJ is larger.

CONCLUSIONS

In over 2000 traversals above the magnetic dip equator the POGO satellites provided measurements of the equatorial electrojet (EEJ) covering -30° to 30° dip latitude, all longitudes round the earth, in the altitude range 400 – 800 km, from about 09 hr to 15 hr local time. This unprecedented coverage of EEJ provides the rare opportunity exploited in this group of papers to present all the 10 possible cross sections of EEJ current.

This paper provides the all-longitude means of 7 local time hours: 09, 10, 11,.....15 hour; and the daytime means for 36 longitudes: 0° , 10° , 20° ,..... 350°E , of the vertical distribution parameters of EEJ current density. These means are the bases of the altitude-local time and altitude-longitude cross sections presented in this paper.

The altitude-local time cross section of EEJ current density has only one big contour cell that peaks at (12 h, 106 km). The altitude-longitude cross section of EEJ current density displays three contour cells peaking at (100°E , 106 km), (190°E , 106 km) and (290°E , 106 km).

The main feature of the two cross sections is that the contour of a given current density extends farther from the altitude of the peak current density at 106 km when the peak current density at the centre of EEJ is larger. Consequently, the altitude-longitude cross section has a wavy character because the altitude of each contour above 106 km altitude has maxima at 100°E , 190°E and 290°E , and minima at 140°E and 230°E ; and vice versa below 106 km altitude.

The above phenomenon is explained. The two rocket observations in its support are cited. It is recalled that by the same phenomenon the contours also extend farther in latitude when the peak current density at the current centre is larger.

From the discussions and comparisons of altitude distribution parameters of EEJ current density from rocket data at India and Peru, and from POGO satellites data, the following conclusions are also reached.

- (a) The continuous distribution of current density model is an excellent model for the reproduction of altitude distribution parameters of EEJ current density.
- (b) The altitude distribution parameters of EEJ current density in India and Peru are not significantly different.
- (c) The altitude distribution parameters of EEJ current density from rockets data and from POGO satellites data are not significantly different.

- (d) However, it is essential to take into account the lack of symmetry between the vertical distributions of EEJ current density below and above the altitude of EEJ peak current density.

REFERENCES

- Cahill L.J.Jr., 1959. Investigation of the equatorial electrojet by rocket magnetometer, *J. Geophys. Res.*, 64: 489 – 503.
- Maynard N.C., 1967. Measurements of ionospheric currents off the coast of Peru, *J. Geophys. Res.*, 72: 1863 – 1875.
- Onwumechili C.A., 1965. A three dimensional model of density distribution of ionospheric current causing part of quiet day geomagnetic variations. Proc. Second International Symposium on Equatorial Aeronomy, pp: 384 – 386, ed. By F. de Mendonca, Brazilian Space Commission, Sao Paulo.
- Onwumechili C.A. 1966. The magnetic field of a current model for part of geomagnetic Sq variations. 11^e Symposium d'aeronomie equatoriale: 163 – 170. A special publication of Annales de Geophysique.
- Onwumechili C.A., 1992a. A study of rocket measurements of ionospheric currents-I. General setting and nighttime ionospheric currents, *Geophys. J. Int.*, 108: 633 – 640.
- Onwumechili C.A., 1992b. A study of rocket measurements of ionospheric currents-II. Ionospheric currents outside the dip equatorial zone, *Geophys. J. int.*, 108: 633 – 640.
- Onwumechili C.A., 1992c. A study of rocket measurements of ionospheric currents-III. Ionospheric currents at the magnetic dip equator, *Geophys. J. Int.*, 108: 647 – 659.
- Onwumechili C.A. 1992d. A study of rocket measurements of ionospheric currents-IV. Ionospheric currents in the transition zone and the overview of the study, *Geophys. J. Int.*, 108: 660 – 672.
- Onwumechili C.A. 1992e. A study of rocket measurements of ionospheric currents-V. Modelling rocket profiles of low latitude ionospheric currents, *Geophys. J. Int.*, 108: 673 – 682.
- Onwumechili C.A. and P.O. Ezema, 1992. Latitudinal and vertical parameters of the equatorial electrojet from an autonomous data set, *J. Atmos. Terr. Phys.*, 54: 1535 – 1544.
- Sastry T.S.G., 1997. Diurnal change in the parameters of the equatorial electrojet as observed by rocket-borne magnetometers, *Space Res.*, X: 778 – 785.